Effects of well width and growth temperature on optical and structural characteristics of AlN/GaN superlattices grown by metal-organic chemical vapor deposition

C. Bayram, N. Péré-laperne, and M. Razeghi[a)]
Department of Electrical Engineering and Computer Science, Center for Quantum Devices, Northwestern University, Evanston, Illinois 60208, USA

(Received 1 September 2009; accepted 3 November 2009; published online 20 November 2009)

AlN/GaN superlattices (SLs) employing various well widths (from 1.5 to 7.0 nm) are grown by metal-organic chemical vapor deposition technique at various growth temperatures (T_S) (from 900 to 1035 °C). The photoluminescence (PL), x-ray diffraction, and intersubband (ISB) absorption characteristics of these SLs and their dependency on well width and growth temperature are investigated. Superlattices with thinner wells (grown at the same T_S) or grown at lower T_S (employing the same well width) are shown to demonstrate higher strain effects leading to a higher PL energy and ISB absorption energy. Simulations are employed to explain the experimental observations. ISB absorptions from 1.04 to 2.15 μm are demonstrated via controlling well width and growth temperature. © *2009 American Institute of Physics*. [doi:10.1063/1.3267101]

Wide-band gap AlN/GaN superlattices (SLs) has a large conduction-band offset[1] (~2.1 eV) suitable for near-infrared intersubband (ISB) devices, and has the potential to offer tunability over the complete optical communications wavelength region (1.2–1.7 μm) for applications including multiterabit optical time division multiplexed networks as well as chemical/biological sensing. Large electron effective mass ($m^* \sim 0.2-0.3 \times m_0$) and longitudinal optical phonon energy (~90 meV) enable ultrafast ISB relaxation promising AlN/GaN SLs as active layers in high-performance ISB devices.[1] However, due to the lack of readily available affordable lattice-matched substrates, the high quality growth of AlN/GaN SLs proves challenging.

Today, most nitride based commercial optoelectronic devices are grown by metal-organic chemical vapor deposition (MOCVD). Thus, there is a wide interest to realize high quality ISB absorption in optical communications wavelengths by MOCVD. Recently, some groups have reported MOCVD-grown AlN/GaN SLs absorbing in near-infrared[2] but only few led to absorption around 1.5 μm (Refs. 3–5) No studies yet can demonstrate ISB absorption at lower wavelengths. In this work, we demonstrate ISB absorption in the complete optical communications wavelength range and correlate the effects of well width and growth temperature on the optical and structural characteristics of AlN/GaN SLs grown by MOCVD.

The material is grown in an AIXTRON 200/4-HT horizontal flow low-pressure MOCVD reactor. The template, consisted of a high quality AlN layer, is grown on double-side polished (001) sapphire.[6] Trimethlyaluminum, trimethylgallium, and trimethlyindium are used as the metalorganic precursors for Al, Ga, and In, respectively. Silane is used as the *n*-type dopant source. Ammonia and hydrogen are used as the anion source and carrier gas, respectively. All SL growths are performed via our pulsed MOCVD technique described in Ref. 7 at a pressure of 50 mbar. For each growth temperature (T_S) (900, 970, and 1035 °C), AlN and GaN growth rates are calibrated prior to SL growths.[7] All SLs are capped with 30-nm-thick AlN.

Room temperature photoluminescence (PL) measurements are realized via frequency doubled argon-ion laser at 244 nm. Figure 1 shows the room temperature PL intensity as a function of wavelength for 50 periods of {1.5-nm-thick GaN/3-nm-thick AlN} grown at three different T_S (900, 970, and 1035 °C). Blueshift in PL wavelength and decrease in PL intensity are observed with decreasing SL growth temperature. Figure 1 inset displays the dependency of PL energy and intensity on GaN well width (for a constant 3.0-nm-thick AlN barrier). Decrease in both PL energy and intensity are observed as well is widened. This PL behavior originates due to strain in the SL. In a strained material, as the well

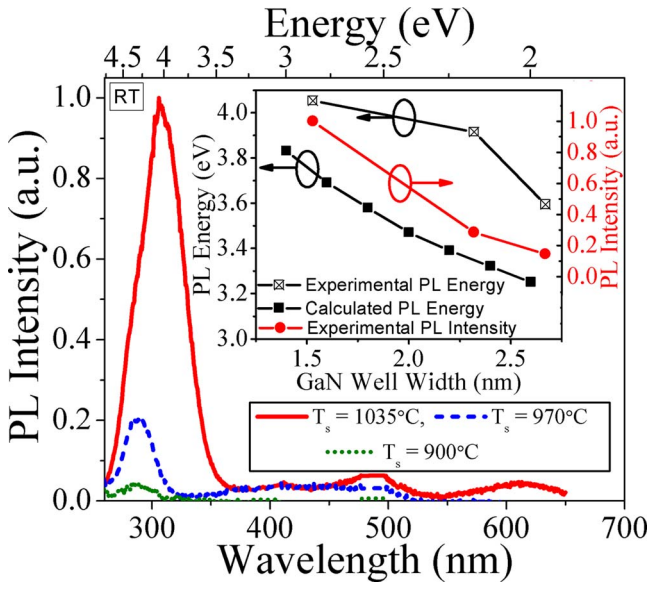

FIG. 1. (Color online) Room temperature PL intensity is plotted as a function of wavelength for three different growth temperatures, 900, 970, and 1035 °C for 50 periods of {1.5 nm thick GaN/3 nm thick AlN}. Wells are *n*-doped to 1×10^{18} cm^{-3}. Inset shows the experimental (and simulated) PL energy as a function of well width [for the same barrier thickness and growth temperature (T_S) of 1035 °C].

a)Electronic mail: razeghi@eecs.northwestern.edu.

width increases, the electron and hole wave functions are confined in the triangular part of the well due to the quantum-confined Stark effect. As a consequence, the overlap between the two wave functions decreases resulting in decreased recombination efficiency and thus PL intensity.

The dependency of PL energy on well width can be explained as follows: The band-edge transition energy (E_{hm}^{en}) is given by $E_{hm}^{en}=E_g+E_{en}-E_{hm}$ where E_g is the bandgap energy, and E_{en} and E_{hm} are nth electron (e) subband, and mth hole (h) subband energy in the presence of electric field (F) that are given by

$$E_{en(hm)} = E^0_{en(hm)} + C_{n(m)} m^*_{e(h)} e^2 F^2 L^4_{eff}/\hbar^2, \quad (1)$$

$$E^0_{en(hm)} = \hbar^2/2m^*_{e(h)}[n(m)\pi/L]^2, \quad (2)$$

$$C_x = (x^2\pi^2 - 15)/(24x^4\pi^4), \quad (3)$$

where E^0_{nx} is the subband energy for $F=0$, m^*_x, e, L_{eff}, and $\hbar$ are effective mass, unit electron charge, effective well width, and reduced Planck constant, respectively.[8] Subband energies are measured from the band-edges at the center of the quantum well (positive for electrons and negative for holes). Therefore, the band-edge transition energy for the first conduction and the first heavy-hole subband is given by $E^{e1}_{h1}(F)=E^{e1}_{h1}(F=0)+C_1(m^*_e+m^*_h)e^2F^2L^2_{eff}/\hbar^2$. Equations (1)–(3) state that PL energy (ex. E^{e1}_{h1}) of a level is inversely proportional to the well width (as shown in Fig. 1 inset). As the well width increases, the electronic and hole bound states get lower which lead to a lower energy between these states. The observed decrease in PL intensity with increasing well width is attributed to the bigger spatial separation of electron and hole wave functions by the (internal) electric field (F). The (internal) electric field, F, originates from the piezoelectric and spontaneous polarization of the AlN–GaN interfaces.

A theoretical model is employed to simulate inter- and intersub-band energy levels to compare with the experimental observations. More details on the theoretical model are given elsewhere.[9] Figure 1 inset displays the experimental and theoretical PL energy as a function of the GaN well width. The interband simulations and PL experiments are in reasonably good agreement, however, a shift in energy between simulation and experiments is observed. This discrepancy of our experimental results with theory can be accounted for strain nonuniformities and interface quality. The simulation assumes a uniform strain across the structure and ignores the partial relaxations (that lead to interfacial roughness) occurring at the AlN–GaN interfaces. Another reason for interface degradation is GaN thinning, which will be addressed in the next sections.

Samples are prepared for ISB absorption measurements by dicing to allow transverse optical access to the layers. p- or s-polarized white light is incident perpendicular to one side facet of the samples, traveled along the SL region and go out from the other facet.[7] The infrared transmission is measured at room temperature using a Fourier transform infrared spectrometer. The difference between the absorption of p- and s-polarized light is used to identify ISB absorption. Figure 2 displays the (p-polarized) transmission of the SLs with well widths of 1.5, 2.2, and 2.7 nm (with AlN barrier width of 3.0 nm). Figure 2 shows that lower T_S results in a higher ISB absorption energy, and a narrower absorption feature. Figure 2 inset shows the effect of T_S and well width on

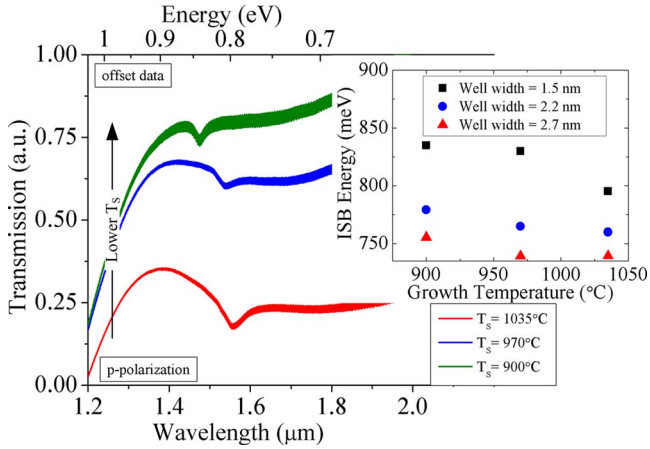

FIG. 2. (Color online) Transmission is plotted as a function of wavelength for three different growth temperatures, 900, 970, and 1035 °C for 50 periods of {1.5 nm thick GaN/3.0 nm thick AlN}. Wells are doped to 1×10^{18} cm^{-3}. Inset shows ISB transition energy as a function of growth temperature for well widths of 1.5, 2.2, and 2.7 nm.

ISB energy. Wider wells and higher T_S lead to lower ISB energies. Wider wells decrease the separation between first and second electronic state leading to lower ISB energy [see Eq. (2)].

X-ray diffraction (XRD) studies are realized by high resolution Panalytical MPD-Pro system. Figure 3 shows the (002) $\Omega/2\theta$ XRD scans of the SLs with different well widths (1.5, 2.7, 4.3, and 7.0 nm) grown at 1035 °C (solid line). For the well widths of 1.5 and 2.7 nm, XRD scans of SLs grown at 900 °C are also plotted. The satellite peaks are narrower for the SLs grown at lower T_S. Figure 3 inset displays the GaN thickness dependency on GaN deposition time. Fifty periods of various SLs are grown, and layer thicknesses are deducted as follows: the angular separation between satellite peaks are used to calculate the SL period.[10] The average aluminum composition is calculated via $x_{Al}=(C_{AlGaN}$

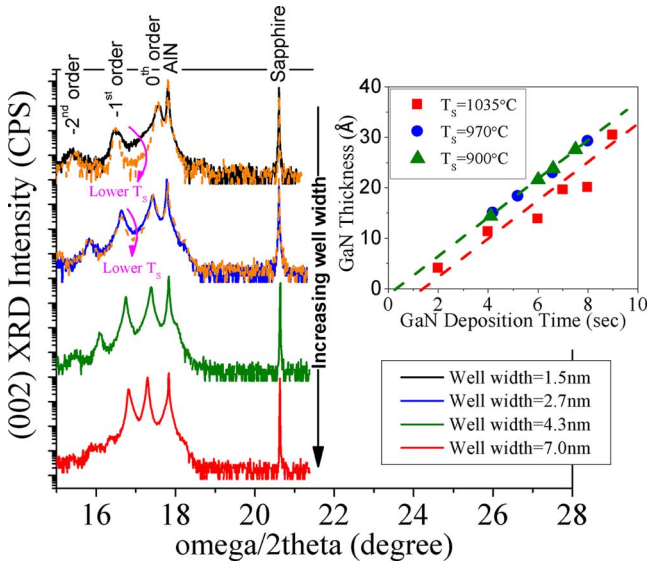

FIG. 3. (Color online) (002) $\Omega/2\theta$ XRD of the SL with four well widths (all n-doped of 1×10^{18} cm^{-3}) of 1.5, 2.7, 4.3, and 7.0 nm, employing 3 nm thick barrier thickness, are plotted. All SL are grown at growth temperature (T_S) of 1035 °C (solid). The XRD of 1.5 and 2.7 nm thick wells grown at 900 °C are also shown (dashed). Inset shows the GaN thickness as a function GaN deposition time for three different growth temperatures, 900, 970, and 1035 °C.

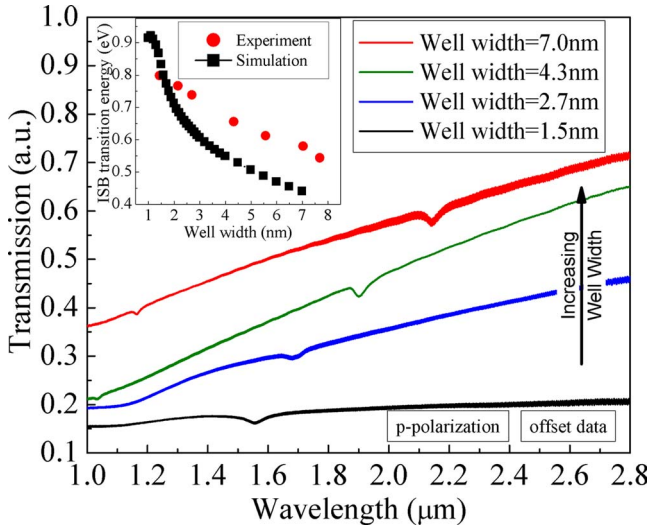

FIG. 4. (Color online) Transmission is plotted as a function of wavelength for four well widths of 1.5, 2.7, 4.3, and 7 nm. For all cases, AlN barrier thickness and growth temperature is 3.0 nm and 1035 °C, respectively. Inset shows simulated and observed ISB absorption energies as a function of well width (for the transition from the first state to the second state where other transitions are possible).

$-C^0_{GaN})/(C^0_{AlN}-C^0_{GaN})$ where C^0_{GaN} and C^0_{AlN} are the free-standing lattice parameters of GaN and AlN, and C_{AlGaN} is the average lattice constant of the SL determined from x-ray analysis.[10] The linear fit to GaN thickness (Fig. 3 inset) at 1035 °C intersect ordinate below abscissa which is attributed to the thinning of the GaN wells at high temperatures while AlN deposition.[11] However, for SLs grown at 900 and 970 °C, linear fit to GaN thickness intersect ordinate almost at origin. These demonstrate that the interface quality is better for SLs grown at lower temperatures, mainly due to decrease in thinning of the GaN wells at lower temperatures. This shows that AlN/GaN SLs grown at lower temperatures have better-defined interfaces. Better-defined interfaces also result in higher strain in the well that agrees with our analysis of PL energy/intensity and ISB absorption energy behavior addressed previously.

Figure 4 displays the (p-polarized) transmission of the SLs with well widths of 1.5, 2.7, 4.3, and 7.0 nm. The absorption feature (attributed to transition from first to second electronic state) redshifts with increasing well width. This is related to electron states getting closer to each other as the well gets wider (see Eq. (2)). For wells of 4.3 and 7.0 nm, another absorption feature with higher energy is observed. This is attributed to the transition from the first to the third electronic state. With the varying well width, ISB absorption (from the first state to second state) is tuned from 1.5 to 2.2 μm, and absorption features (from the first state to third electronic state transitions) as low as 1.04 μm are realized.

The ISB absorption wavelength as a function of well width is simulated;[9] a comparison with the experimental data is shown in Fig. 4 inset. The simulation data is in a good harmony with the experimental one for thinner wells, however, as the well width increases, simulated, and experimentally measured ISB energies begin to differ. This could be attributed to degradation in SL quality for widest wells. When XRD scans of SLs with 1.5–7.0 nm thick wells are compared (in Fig. 3), it is noticed that satellite peaks get narrower from 1.5 to 4.3 nm thick ones, but degrades for the 7.0 nm thick one. This is related to growing GaN thicker than critical thickness in AlN/GaN SL.[12] The discrepancy of our experimental data with the simulation one can be accounted for strain nonuniformities along the SL and in the interface quality of the SL.

In summary, SLs with thinner wells (grown at the same T_S) or grown at lower T_S (employing the same well width) demonstrate higher strain effects leading to a higher PL energy and ISB absorption energy. The higher strain effects in SLs with thinner wells and SLs grown under lower T_S are attributed to higher well quality (due to growing thinner than critical thickness) and less thinning of the GaN well (due to less etching effect of Al adatoms). Well width and the growth temperature are shown to be key parameters for AlN/GaN SLs absorbing in optical communications wavelengths. Theoretical analysis and simulations are realized to explain experimental observations.

The authors would like to thank Dr. R. McClintock from Center for Quantum Devices at Northwestern University for assistance in measurement setup, Dr. D. Silversmith of the AFOSR, Dr. H. Temkin, and Dr. M. Rosker of DARPA, and Dr. J. Zavada of ARO for their support and encouragement.

[1] I. Vurgaftman and J. R. Meyer, J. Appl. Phys. **89**, 5815 (2001).
[2] I. Waki, C. Kumtornkittikul, Y. Shimogaki, and Y. Nakano, Appl. Phys. Lett. **82**, 4465 (2003); **84**, 3703 (2004).
[3] E. Baumann, F. R. Giorgetta, D. Hofstetter, S. Golka, W. Scherenk, G. Strasser, L. Kirste, S. Nicolay, E. Feltin, J. F. Carlin, and N. Grandjean, Appl. Phys. Lett. **89**, 041106 (2006).
[4] S. Nicolay, E. Feltin, J.-F. Carlin, N. Grandjean, L. Nevou, F. H. Julien, M. Schmidbauer, T. Remmele, and M. Albrecht, Appl. Phys. Lett. **91**, 061927 (2007).
[5] H. Sodabunlu, J.-S. Yang, M. Sugiyama, Y. Shimogaki, and Y. Nakano, Appl. Phys. Express **2**, 061002 (2009).
[6] C. Bayram, J. L. Pau, R. McClintock, and M. Razeghi, J. Appl. Phys. **104**, 083512 (2008).
[7] C. Bayram, N. Péré-laperne, R. McClintock, B. Fain, and M. Razeghi, Appl. Phys. Lett. **94**, 121902 (2009).
[8] S. L. Chuang, *Physics of Optoelectronic Devices* (Wiley, New York, 1995).
[9] N. Péré-Laperne, C. Bayram, L. Nguyen-Thê, R. McClintock, and M. Razeghi, Appl. Phys. Lett. **95**, 131109 (2009).
[10] S. Zhou, M. F. Wu, S. D. Yao, B. S. Zhang, and H. Yang, Superlattices Microstruct. **40**, 137 (2006).
[11] N. Gogneau, D. Jalabert, E. Monroy, E. Sarigiannidou, J. L. Rouviere, T. Shibata, M. Tanaka, J. M. Gerard, and B. Daudin, J. Appl. Phys. **96**, 1104 (2004).
[12] A. D. Bykhovski, B. L. Gelmont, and M. S. Shur, J. Appl. Phys. **81**, 6332 (1997).